Evidence of strong projectile–target-core interaction in single ionization of neon by electron impact

S. Yan,[1,2] X. Ma,[1,*] P. Zhang,[1,2] S. Xu,[1,2] S. F. Zhang,[1] X. L. Zhu,[1] W. T. Feng,[1] and H. P. Liu[1]

[1]*Institute of Modern Physics, Chinese Academy of Sciences, Lanzhou 730000, China*

[2]*Graduate School of Chinese Academy of Sciences, Beijing 100049, China*

(Received 14 September 2010; published 3 November 2010)

The momentum distributions of recoil ions were measured in the single ionization of neon by electron impact at incident energies between 80 and 2300 eV. It was found that there are a noticeable number of recoil ions carrying large momenta, and the relative contributions of these ions becomes more pronounced with the further decrease of incident electron energy. These observed behaviors indicate that there is a strong projectile–target-core interaction in the single-ionization reaction. By comparing our results with those of electron-neon elastic scattering, we concluded that the elastic scattering of the projectile electron on the target core plays an important role at low and intermediate collision energies.

DOI: 10.1103/PhysRevA.82.052702 PACS number(s): 34.80.Dp

I. INTRODUCTION

The study of electron-impact single ionization of atoms and molecules, namely, the $(e,2e)$ reaction, is of fundamental importance for our understanding of few-body quantum dynamics [1]. This process also plays a key role in various plasma phenomena. Since the pioneering work of Ehrhardt *et al.* [2], numerous studies on $(e,2e)$ dynamics, both experimental and theoretical, have been carried out.

Most of the experiments focused on the coplanar asymmetric geometry for which the state-of-the-art theoretical models, such as Brauner-Briggs-Klar [3], convergent close coupling (CCC) [4], and distorted-wave Born approximation (DWBA) [5], could satisfactorily reproduce experimental results, especially for simple targets. Besides, in order to get a better insight into the collision dynamics and, in particular, into the role of higher-order effects in the projectile-target interaction, other collision geometries were also explored.

Concerning the role of the higher-order effects in $(e,2e)$ reactions, one has to note that most of the previous work, devoted to this topic, was focusing on simple targets such as helium and atomic hydrogen. Byron *et al.* [6] predicted an interesting behavior of the triple-differential cross sections (TDCS) for single ionization of H($1s$) under coplanar symmetric geometry, that is, in the case where both outgoing electrons move in the scattering plane and with symmetric angles with respect to the projectile axis. This was done in [6] by including the second Born term in the calculation. According to Byron's results, the second Born term can be interpreted as describing a two-step process in which the incident electron, in addition to the interaction with the bound electron, also experiences an elastic scattering on the target core. Pochat *et al.* [7], Frost *et al.* [8], and Gelebart and Tweed [9] measured the TDCS for single ionization of He($1s^2$), their results were in agreement with Byron's prediction.

In the work of Murray *et al.* [10], the case of out-of-plane geometry was considered. Here, both outgoing electrons with equal energy were detected in a plane perpendicular to the direction of the incoming electron beam. For such geometry it was found that maxima arise in the cross section at angles of 90°, 180°, 270° between the emitted and the scattered electrons. The origin of these maxima was explained by Zhang *et al.* [11,12] as appearing due to the two-step process mentioned earlier. In another experiment with the same geometry, Al-Hagan *et al.* [13] investigated the TDCS of the $(e,2e)$ reactions on He and H_2 targets for low-energy electron impact. They found large differences between $(e,2e)$ on He and H_2 and explained them based on the two-step process which proceeds in these two cases differently because of the different nuclear field.

It is known that the role of the higher-order effects becomes more important when the atomic number Z increases. Therefore, in order to explore these effects, the exploration of $(e,2e)$ on heavy atomic targets is highly desirable. However, there are only a few recent experimental studies focusing on this issue. Van Boeyen *et al.* [14] performed the Mg $(e,2e)$ experiment, the results of which were in good agreement with DWBA calculation including elastic scattering of the incident electron on the target core. Ren *et al.* [15] measured the three-dimensional TDCS for Ar $(e,2e)$. The authors compared the TDCS in the scattering plane and in the plane that contains the vector of projectile beam and is perpendicular to scattering plane. They found some similarities in Ar $(e,2e)$ for these two planes and explained them by using the two-step mechanism mentioned previously.

All the previous studies devoted to exploration of the higher-order effects in $(e,2e)$ reaction chose particular collision geometries and specific energies of the emitted and scattered electrons and were always focused on the characteristics of the electrons. Such studies can yield very detailed information on the $(e,2e)$ process and, in particular, on the role of the interaction between the projectile electron and the target core in this process. However, because of the "highly differential" character of such information, it is quite difficult to obtain the general overview of the process under consideration from these studies. The question, therefore, arises as to whether one can find a way that would enable one to obtain more integral and compact characteristics of the $(e,2e)$ process and, in particular, the projectile–target-core interaction without the necessity of considering very many collision geometries.

In the present article we show that such characteristics can, in fact, be obtained by exploring momentum spectra of

*x.ma@impcas.ac.cn

the target recoil ions (note that in our present experimental arrangement we can detect the momenta of the target recoil ions with an efficiency of 100% covering the whole 4π solid angle). Indeed, the strong interaction between the projectile electron and the target core can manifest itself by large momentum transfer to the recoil ion which might be visible in the ion spectra. Moreover, since instead of considering two particles—the scattered and the emitted electrons—the attention will be focused just on one particle—the recoil ion, there will be fewer degrees of freedom and thus one may hope to get more compact and complementary information about the ionization process.

Taking what has been said previously into account, in this article we investigate the single ionization of Ne($2p^6$) in collisions with electrons by measuring the recoil ion momentum. For these measurements we used the longitudinal reaction microscope at the Institute of Modern Physics (Lanzhou). Energies of the incident electrons were varied between 80 and 2300 eV. The momentum vector of the recoil Ne^+ was reconstructed and used to generate singly differential cross sections (SDCSs). The SDCS of the ionization process is compared with the case of electron-neon elastic scattering. The present study, in particular, demonstrates that the relative contribution of large longitudinal momenta increases when the impact energy decreases and that in the Ne (e,2e) reaction the scattering of the projectile on the target ion core to angles larger than 90° (backward scattering) becomes important at low and intermediate energies.

Atomic units (a.u.) are used throughout unless indicated otherwise.

II. EXPERIMENT

The experiment was performed using a longitudinal reaction microscope. The experimental setup is shown in Fig. 1. A pulsed electron beam with a pulse width of 20 ns at 12 kHz repetition rate is used in the experiment. After being confined by a uniform magnetic field (**B**) of 5 G produced by a pair of Helmholtz coils, the pulsed electron beam collides with the Ne target produced in a two-stage supersonic gas jet. The produced Ne^+ ions are extracted and accelerated by the electrostatic field **E** (0.5 V/cm). Then the ions go through the field-free drift region and finally hit on the position-sensitive detector equipped with a delay-line anode. The recoil ion detector is located beneath the electron beam, as shown in Fig. 1. The position and the time-of-flight information were recorded event by event by a PXI-based data-acquisition system. The residual beam is collected into a Faraday cup. Later, in off-line data analysis, the momentum vector of the recoil ions can be reconstructed [16]. The resolution of the longitudinal momentum is estimated to be 0.4 a.u..

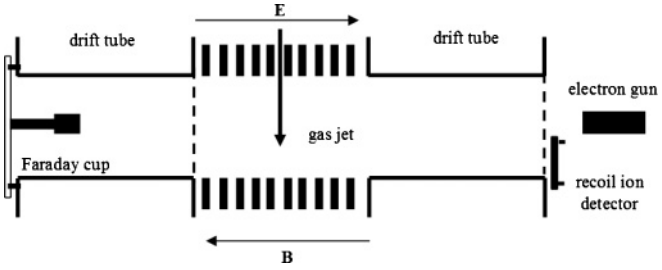

FIG. 1. Schematic view of the experimental setup.

III. RESULTS AND DISCUSSIONS

In Fig. 2 the two-dimensional spectra of the recoiling Ne^+ ion are presented for electron impact energies of 2300, 220, 180, 144, 110, and 80 eV, respectively. The abscissa is the longitudinal momentum ($q_\parallel$) and the ordinate is the transverse momentum ($q_\perp$).

Inspecting these plots in Figs. 2(b)–2(f) unveils that there are the following four interesting features in the momentum spectra of the recoil ions. First, the momentum distributions have a similar shape, which is like a semicircle strip [see the space included by the solid line in Fig. 2(c)]. Second, most of the recoil ions have relatively small momentum with their distributions peaking around $q_\parallel = 0$. Third, there are also a noticeable number of recoil ions which carry large momenta, with the maximum value of the longitudinal momentum being about twice the initial momentum of the projectile electron. Fourth, when the energy of the incident electron decreases, an additional (second) maximum appears at large longitudinal momentum $q_\parallel$. This maximum becomes more pronounced when the projectile energy decreases further.

We note that in the case of very energetic projectiles (2300 eV) the spectrum of recoil only has a maximum peaking around $q_\parallel = 0$, in particular, the spectrum does not spread to the range of large momenta [see Fig. 2(a)].

In order to interpret our experimental results, we first consider the scheme of two-body kinematics [17] for elastic scattering, which is shown in Fig. 3. In this figure, k_0, k_a, and K denote the initial momentum of the projectile, the momentum of the scattered projectile, and the momentum transfer (the recoil momentum), respectively. θ is the scattering angle. For the two-body elastic scattering, the sum of the momenta of the scattered electron and the target must be equal to the initial momentum k_0, that is, $k_0 = k_a + q$, $K = k_0 - k_a = q$. Thus, the momentum of the recoil target will always lie on the semicircle centered at (k_0, 0) with radius equal to

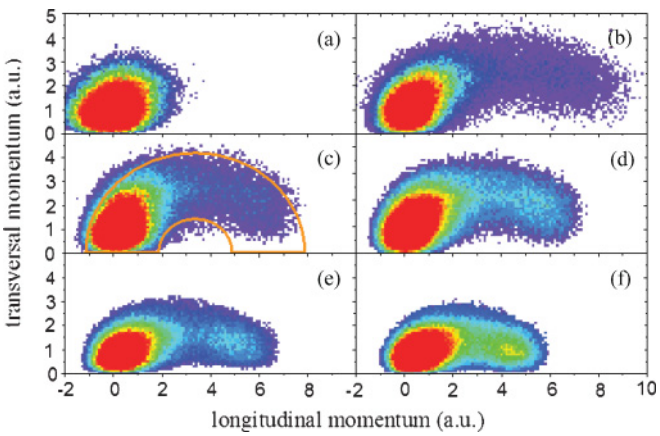

FIG. 2. (Color online) The momentum distributions for Ne^+ recoil ions. The x coordinate represents the longitudinal momentum and y coordinate represents the transversal momentum. The incident electron energies are (a) 2300 eV, (b) 220 eV, (c) 180 eV, (d) 144 eV, (e) 110 eV, and (f) 80 eV.

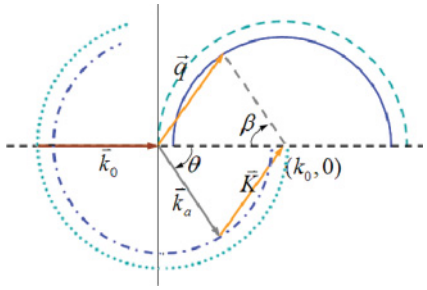

FIG. 3. (Color online) Sketch of the two-body collision kinematics.

k_0 (the dashed-line semicircle in Fig. 3). For an inelastic scattering, in which the target undergoes a transition into an excited bound state, the recoil momentum, because of energy losses, will be aligned on the semicircle with reduced radius (the solid-line semicircle in Fig. 3). The scattering angle θ can be deduced from the momentum vectors of the recoil target and the projectile (see Fig. 3). In general, the recoil target has largest transverse momentum at $\theta = 90^o$, small longitudinal and transverse momentum when θ approaches 0°, and large longitudinal momentum and small transverse momentum when θ approaches 180°.

For single ionization there are three particles in the final state: the recoil ion, the scattered and emitted electrons. Now one has $k_0 = k_a + k_b + q$, where k_b is the momentum of the ejected electron, and there is no simple kinematical scheme similar to that for elastic scattering.

The recoil ion momentum can be written as $q = k_0 - k_a - k_b = K - k_b$. It is obvious that, due to a nonzero value of k_b, the recoil ion momenta, instead of lying on a semicircle curve, will distribute in a semicircle strip [like the space defined by the solid line in Fig. 2(c)]. This observation may explain the shape and the broadness of the distribution of the recoil ion momentum, which is shown in Fig. 2. For a further analysis of the momentum spectra of the recoil ions in the $(e,2e)$ reaction, we define a new momentum vector $k_s = k_a + k_b$. The direction of the momentum vector k_s can be characterized by the angle β (see Fig. 3). If in the final state the emitted electron carries a very small momentum, we have $\beta \approx \theta$, and the $(e,2e)$ kinematics can be approximated by the two-body one for inelastic scattering corresponding to target excitation.

Taking into account that $\cos\beta = (k_0 - q_\parallel)/\sqrt{(k_0 - q_\parallel)^2 + q_\perp^2}$, one can show that in the momentum distributions of Fig. 2 there is a minimum at angles β close to 95°. Besides, the second maximum appears at β larger than 160°, which corresponds to a very large longitudinal momentum of the recoil ions, meaning that we deal with backward scattering. If in our $(e,2e)$ reaction the target core would be just a spectator, and only the interaction between incident electron and the target electron would be efficient, then the backward scattering would be very unlikely to occur. Therefore, we think that the second maximum at large longitudinal momentum reflects the strong interaction between the incident electron and the target core.

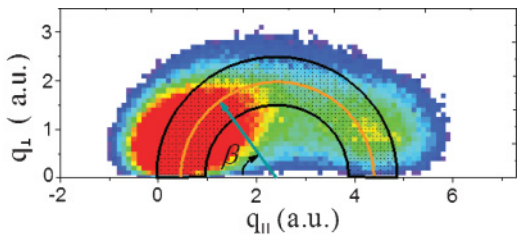

FIG. 4. (Color online) The area used to calculate the differential cross section $(\frac{d\sigma}{\sin\beta d\beta})$ as a function of β angle.

In order to understand the reason for the appearance of the minimum at $\beta \approx 95^\circ$ and the relative increase of backward scattering into the ionization cross section, let us explore the cross-section differential in β. This cross section is calculated by selecting recoil ion momenta in a circular strip (shaded area shown in Fig. 4). The circular strip includes the space between two circles with radii equal to $k \pm \Delta$, where k is the momentum vector of the scattered electron, whose energy loss is taken (somewhat arbitrarily) to be equal to 27 eV, and $\Delta = 0.5$ a.u.. The latter choice was made in order to select enough ionization events from the momentum range where the cross section (along the radius) varies quite smoothly.

The singly differential cross sections $(\frac{d\sigma}{\sin\beta d\beta})$ as a function of β for ionization of neon by incident electrons with energies of 220, 144, and 110 eV are shown in Figs. 5(a), 5(b), and 5(c), respectively. For a comparison in Figs. 5(d), 5(e), and 5(f) we show the singly differential cross section $(\frac{d\sigma}{\sin\theta d\theta})$ as a function of scattering angle θ for the case of elastic e-Ne scattering for impact energies of 200, 150, and 100 eV, respectively. The data for these cross sections were taken from [18,19].

According to Figs. 5(a) and 5(d), the cross sections for ionization by the impact of 220 eV incident electrons and for elastic scattering of 200 eV electrons both have maximum at zero angle, then decrease when the angle increases reaching minima at angles close to 90°. With a further increase in the angles, the cross sections begin to increase. Thus, both cross sections demonstrate rather similar behavior. In particular, for both cross sections the ratio between the backward scattering and the total scattering is similar.

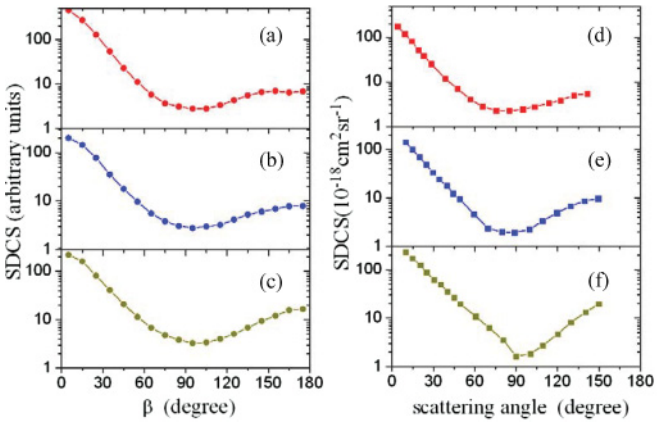

FIG. 5. (Color online) Singly differential cross section for electron-neon elastic scattering and ionization. (Left column) SDCS $(\frac{d\sigma}{\sin\beta d\beta})$ for ionization process as a function of β. The incident electron energies are (a) 220 eV, (b) 144 eV, and (c) 110 eV, respectively. (Right column) SDCS $(\frac{d\sigma}{\sin\theta d\theta})$ for elastic scattering. The incident electron energies are (d) 200 eV, (e) 150 eV, and (f) 100 eV, respectively.

When the energy of the incident projectile decreases [see Figs. 5(b), 5(e) and 5(c), 5(f)], the positions of the minima in the cross sections keep almost unchanged and the relative contribution of the backward scattering becomes more important, for both ionization and elastic scattering. We observe in the figures that the similarities in the ionization and elastic cross sections remain at all the different impact energies.

We believe that the similarities between our results and the results for the elastic scattering may be attributed to the interaction between the projectile and the target core, which in the case of ionization occurs simultaneously with the interaction between the projectile and the active target electron. Thus, in $(e,2e)$ reactions involving heavy atoms the elastic scattering of the projectile electron on the target core plays an important role at low collision energies.

For more insight we also performed an experiment on single ionization of helium by 150 eV incident electrons. In this case, however, there was no minimum for the cross section and the scattering to large angles was strongly suppressed. Note that a similar behavior is known to take place for e-He elastic scattering [20].

One has to add that, besides the previously discussed similarities between the cross sections for ionization and elastic scattering, there are also certain differences between them. For instances, in the case of elastic scattering, when the energy of the incident electrons decrease, the position of the minimum of the cross sections shifts to large angles [comparing Fig. 5(d) to Figs. 5(e) and 5(f)]. In contrast, the position of the minimum in the case of Ne $(e,2e)$ is practically unchanged when the energy of the incident electron varies. Additionally, in the case of elastic scattering the minimum becomes deeper and narrower. For ionization, however, the width and the depth of the minimum are almost energy independent.

IV. SUMMARY

The dynamics of the single ionization of Ne by electron impact for incident energies ranging from 80 to 2300 eV has been explored by measuring the recoil-ion momentum. The measured recoil-ion momentum distributions provided us a more general overview of this ionization process. It was found that at lower impact energies there appear two maxima in the two-dimensional momentum distribution of the recoil ions. One of them is located in the region of small recoil momenta, corresponding to small scattering angles. The other one arises in the region of large longitudinal momenta and corresponds to backward scattering. The relative contribution of this second maximum into the cross section becomes larger when the energy of the incident electron decreases.

We have compared our results for single ionization of neon by electron impact with data on electron-neon elastic scattering. This comparison shows that there are important similarities in the cross sections of these two processes. This allows one to interpret our results for Ne $(e,2e)$ as displaying an important role played in single ionization of neon by the interaction between the electron and the target core. In particular, at lower impact energies this interaction becomes so strong that a noticeable part of the incident electrons experiences scattering to angles larger than 90°. In order to get a better insight into the collision dynamics in the case of backward-scattering angles, further studies such as the exploration of the outgoing electrons are required.

ACKNOWLEDGMENTS

This work is supported by the National Natural Science Foundation of China under Grants No. 10979007 and No. 10674140. The authors thank A. B. Voitkiv for helpful discussions.

[1] A. Lahmam-Bennani, J. Phys. B **24**, 2401 (1991).
[2] H. Ehrhardt, M. Schulz, T. Tekaat, and K. Willmann, Phys. Rev. Lett. **22**, 89 (1969).
[3] M. Brauner, J. S. Briggs, and H. Klar, J. Phys. B **22**, 2265 (1989).
[4] I. Bray and D. V. Fursa, Phys. Rev. A **54**, 2991 (1996).
[5] S. Jones and D. H. Madison, Phys. Rev. A **62**, 042701 (2000).
[6] F. W. Byron Jr., C. J. Joachain, and B. Piraux, J. Phys. B **16**, L769 (1983).
[7] A. Pochat, R. J. Tweed, J. Peresse, C. J. Joachain, B. Piraur, and F. W. Byron Jr., J. Phys. B **16**, L775 (1983).
[8] L. Frost, P. Freienstein, and M. Wagner, J. Phys. B **23**, L715 (1990).
[9] F. Gelebart and R. J. Tweed, J. Phys. B **23**, L641 (1990).
[10] A. J. Murray, M. B. J. Woolf, and F. H. Read, J. Phys. B **25**, 3021 (1992).
[11] X. Zhang, C. T. Whelan, and H. R. J. Walters, Z. Phys. D **23**, 301 (1992).
[12] M. Brauner and J. S. Briggs, J. Phys. B **26**, 2451 (1993).
[13] O. Al-Hagan, C. Kaiser, D. Madison, and A. J. Murray, Nat. Phys. **5**, 59 (2009).
[14] R. W. van Boeyen, N. Watanabe, J. W. Cooper, J. P. Doering, J. H. Moore, and M. A. Coplan, Phys. Rev. A **73**, 032703 (2006).
[15] X. G. Ren, A. Senftleben, T. Pflüger, A. Dorn, K. Bartschat, and J. Ullrich, J. Phys. B **43**, 035202 (2010).
[16] S. P. Cao, X. Ma, A. Dorn, M. Dürr, and J. Ullrich, Acta Phys. Sin. **56**, 6386 (2007).
[17] O. Jagutzki, L. Spielberger, R. Dörner, S. Nüttgens, V. Mergel, H. Schmidt-Böcking, J. Ullrich, R. E. Olson, and U. Buck, Z. Phys. D **36**, 5 (1996).
[18] J. F. Williams and A. Crowe, J. Phys. B **8**, 2233 (1975).
[19] S. C. Gupta and J. A. Rees, J. Phys. B **8**, 417 (1975).
[20] D. F. Register, S. Trajmar, and S. K. Srivastava, Phys. Rev. A **21**, 1134 (1980).